Chapter XX

The use of ERE-Luc reporter mice to monitor estrogen receptor transcriptional activity in a *spatio*-temporal dimension.

Sara Della Torre[1,*], Elisabetta Vegeto[1] and Paolo Ciana[2]

[1]University of Milan, Department of Pharmaceutical Sciences, Via Giuseppe Balzaretti 9, 20133 Milan, Italy.

[2]University of Milan, Department of Health Sciences, Via Antonio di Rudinì, 20142 Milan, Italy.

*Corresponding Author. Email: sara.dellatorre@unimi.it. Tel: +39-02-50318375. Fax: +39-02-50318284

Summary

In spite of the fact that women spend 1/3 of their lives in post-menopause, the search for appropriate therapies able to counteract the derangements associated with the menopause still represents a sort of sought after the “Holy Grail”.

Nowadays, the combination of estrogens and selective estrogen receptor modulators (SERMs) - a class of compounds with a mixed agonist/antagonistic activity on the estrogen receptor (ER) in various tissues – represents the most promising approach to improve post-menopausal women’s health, by preserving the benefits while avoiding the side-effects of estrogen-based therapy.

Given their complex mechanism of action, the evaluation of SERMs activity in combination with conjugated estrogens (CE) requires a multifactorial analysis that takes into account the multifaceted and dynamic effects of these compounds in target tissues, even in relation to the physiological/pathological status.

To accomplish such a goal, we took advantage of the ERE-Luc model, a reporter mouse that allows the monitoring of ER transcriptional activity in a *spatio*-temporal dimension. Cluster analyses performed on *in vivo*/*ex vivo* bioluminescence (BLI) data and *ex vivo* luciferase activity enabled to sustain the combination of CE *plus* bazedoxifene (TSEC, tissue selective estrogen complex) as a valuable option for the pharmacological treatment of the post-menopause.

Key words: estrogen receptors, menopause, hormone replacement therapies, selective estrogen receptor modulators (SERMs), reporter mice, luciferase, imaging *in vivo*, clustering analysis.

1. Introduction

The loss of the regulatory action of estrogens with menopause makes women more susceptible to the risk of developing osteoporosis, cardiovascular diseases (CVDs) and metabolic disorders, such as the metabolic syndrome (MetS), non-alcoholic fatty liver disease (NAFLD) and diabetes [1–5]. In particular, the impaired estrogen signaling in the liver - one of the main estrogen target tissues [6] – leads to a dysregulation of hepatic metabolism and to liver lipid deposition [7], thus promoting the development of NAFLD and the associated extra-hepatic diseases [2,3,8].

The lack of estrogens also impairs brain functions, quickening the cognitive decline and dementia associated with the aging process [9–11] as well as increasing the risk of developing neuro-inflammatory and neurodegenerative diseases [12–15].

Therapies aimed at counteracting menopause-associated disorders should be considered as a main goal to reach for aging women. At present, however, there is no consensus on which hormone replacement therapy (HRT) is more efficacious and devoid of side effects to treat the wide range of disorders that menopause brings along [1,16]. This scenario is a heritage of large, poorly randomized studies, such as the Women's Health Initiative (WHI), that gave misleading results and raised skepticism towards the use of HRT [17]. Indeed, initial reports suggesting that estrogen-based HRT may increase the risk of health adverse effects discouraged women from taking HRT and pharmaceutical companies from developing drugs that counteract the discomforts and disorders associated with the menopause [17,18].

A more recent re-analysis of the WHI trial data demonstrated that benefits and risks of HRT are strongly dependent on the timing of therapy administration: according to this “timing hypothesis”, HRT is considered beneficial when started within 10 years after the onset of menopause and harmful when started after 10 years or in women older than 60 years of age [5,19].

Given this “window of opportunity” and the wide range of disorders associated with menopause, the current position of many endocrine societies is that HRT should be individualized and based on the evaluation of the risk:benefit *ratio*, in order to reduce any related side-effect [16,19–21].

In this context, current research is still focused on the development of safer pharmacological treatments that, while mimicking ER activation, at the same time avoid adverse effects by preventing or limiting the undesired activation of ER in specific tissues, e.g. the reproductive tissues where ER over-activation might favor the development of breast and ovarian cancer.

A valuable approach to improve post-menopausal women's health could be represented by the pharmacological use of selective estrogen receptor modulators (SERMs) [5,22].

SERMs are synthetic non-steroidal compounds showing a mixed agonist/antagonistic activity toward estrogen receptors (ERα and/or ERβ) in target cells, exerting tissue-specific estrogen- or antiestrogen-like actions. Like any estrogenic molecule, SERMs directly bind to ERs (α and/or β), which undergo structural modifications, dissociate from heat shock proteins (HSPs), and directly bind to Estrogen Responsive Element (ERE) in the regulatory promoter regions of target genes, thus promoting or inhibiting their transcription through the interaction with co-activators or co-repressors, respectively [23,24]. SERMs may exert their mixed agonist/antagonistic activity by triggering ER conformational changes, resulting in a variety of specific interactions with other proteins, including co-regulators, other transcription factors or second messengers. SERMs may also regulate the activity of membrane bound G protein-coupled receptor GPR30 [25,26].

In spite of their potential of action, for years the clinical use of SERMs was limited to Raloxifene (RAL), the only compound approved by FDA for the its ability to prevent both breast cancer and osteoporosis; by converse, other SERMs resulted to exacerbate, rather than alleviate the menopausal symptoms, especially the vasomotor symptoms [27].

In virtue of their mixed agonist/antagonistic estrogenic activity, SERMs could enhance estrogenic benefits in certain tissues (i.e. bone and serum lipids) and minimize estrogenic risks in other tissues (i.e. breast tissue and uterus) when administered in combination with estrogen-based therapy. As a proof of concept, bazedoxifene (BZA), a SERM showing favorable effects on bone metabolism and lipid profiles, was tested in combination with conjugated estrogens (CE), the most widely studied and utilized HRT. The term TSEC (tissue selective estrogen complex) was chosen for this combined

therapy (CE/BZA) to define its tissue-selective activity, that resulted to be different from that of either component alone as well as from that of traditional estrogen/progestin therapy.

In the last years, the use of ERE-Luc reporter mice has represented an invaluable tool to analyze ER activation in physiological conditions [6,28] and to monitor in a *spatio*-temporal dimension the efficacy of new drugs in the search of an 'ideal' HRT [29–31]. The ERE-Luc mouse was engineered with the random integration of a construct containing multiple ERE sequences driving the gene encoding the firefly luciferase flanked by insulator sequences that protect the construct from the influences of the surrounding chromatin and ensure the ubiquitous expression of the transgene in all cells [32]. Therefore, the activity of the luciferase (the protein "reporter") can be easily detected and quantified in this bioluminescent reporter model by *in vivo* and *ex vivo* imaging, giving a reliable measure of ER transcriptional activity. The ERE-Luc mouse was shown to be well suited for the *spatio*-temporal study of ER transcriptional activity *in vivo*, by enabling the screening and identification of compounds acting on ERs, and limiting the number of animals to be used in a long-term study, in accordance with the **3R** philosophy (**R**educe, **R**eplace, **R**efine) [33].

In this chapter we describe standard protocols used to assess the efficacy of TSEC as a potential HRT, by evaluating in different districts to which extent the long-term (21 days) administration of TSEC reinstates the physiological ER signaling, that is typical of fertile females with a regular estrous cycle (Cyc), when used in post-menopause-like conditions (surgical ovariectomy, OVX).

The effects of the combined therapy CE/BZA were evaluated by comparing the ER signaling measured in OVX female mice treated with TSEC with that measured in OVX female mice treated with CE or BZA. In view of its well-known activity in some tissues, RAL was also introduced in the long-term study as a benchmark. The assessment of TSEC efficacy was achieved by performing a cluster analysis of all the data obtained by *in vivo* and *ex vivo* imaging analysis.

2. Material

2.1 Mice and diet

1. Heterozygous C57BL/6 ERE-Luc females [32]. See also **Note 1**.
2. Estrogen-free diet (e.g., 4RF21 from Mucedola; see also **Note 2**).

2.2 Mice treatments

1. Tween 80.
2. Carboxymethylcellulose.
3. Dimethyl Sulfoxide (DMSO).
4. Conjugate estrogens (CE, from Wyeth).
5. Bazedoxifene (BZA, from Wyeth).
6. Raloxifene (RAL, from Wyeth).
7. 0.3 mL syringes with 30G needles.
8. 1 mL syringes.
9. Mouse feeding tubes—plastic or metal.
10. Hamilton syringe (75N, volume 5 μL, needle size 26s ga).

2.3 *In vivo* and *ex vivo* bioluminescence imaging

1. Luciferin: D-luciferin powder (beetle luciferin potassium salt, from Promega) resuspended 25 mg/mL in ultrapure H_2O.
2. Isoflurane gaseous anesthesia equipment including gas vaporizer, scavenger, and oxygen generator (e.g., XGI-8 Gas Anesthesia System connected to an oxygen tank or generator).
3. *In vivo* bioluminescence imaging system (e.g., IVIS series, from PerkinElmer).
4. Micro-dissection tools, including forceps, scissors, and blades.

5. Brain matrix sectioning device for adult mouse, coronal and sagittal, 1 mm spacing (see also **Note 3.**).

2.4 Luciferase enzymatic assay

1. K_2HPO_4
2. KH_2PO_4
3. $(MgCO_3)_4Mg(OH)_2*5H_2O$
4. Ethylenediaminetetraacetic acid (EDTA)
5. Tricin
6. $MgSO_4*7H_2O$
7. 1,4-Dithiothreitol (DTT).
8. Ethylene glycol-bis(2-aminoethylether)-*N,N,N′,N′*-tetraacetic acid (EGTA).
9. Luciferin: D-luciferin powder (beetle luciferin potassium salt, from Promega)
10. Tissue homogenizer (e.g. TissueLyser Qiagen, with 5mm inox beads and bead dispenser).
11. White (not transparent) 96-well microplates.
12. Microplate luminometer (e.g., GloMax®, Promega).
13. Bradford Protein Assay Kit, including protein standards.
14. Transparent 96-well microplates.
15. Microplate absorbance reader.

2.5 General items

1. 20 µL, 200 µL, 1000 µL single pipettors.
2. 20 µL and 200 µL multichannel pipettors.
3. 2 mL microcentrifuge tubes (e.g., Eppendorf® Safe-Lock tubes)
4. 15 mL and 50 mL tubes.
5. Refrigerated microcentrifuge.

6. Bidistilled H_2O to prepare all the solutions; ultrapure H_2O (i.e. MilliQ) to dilute all the compounds for HRT.

2.6 Analysis of imaging data and statistical analysis

1. Software for imaging data analysis and visualization. Imaging workstations and luminometers include proprietary software to operate the devices and allow the direct export of raw data.
2. Software for data analysis and statistical analysis. Many statistical programs could be used to analyze the data (e.g. GraphPad Prism).

3. Methods

3.1. *In vivo* imaging set-up: luciferase substrate distribution.

Time-course study (see also **Note 4**):

1. Anesthetize 3 reporter mice (see also **Note 5**) by gas anesthesia by exposing mice for 2 min to isofluorane (see also **Note 6**).
2. Inject mice intraperitoneally (i.p.) with 80 mg/kg D-luciferin (see also **Note 7**).
3. After having taken a photo of the mice in dimmed light, measure photon emission with a series of 5 min imaging sessions. Generally, photon emission is maximal between 10 and 25 min after the i.p. injection and then gradually decreases.
4. At the end of the imaging section (see **Note 8**), perform data analysis by measuring with the dedicated software (e.g., Living Image Software for IVIS series from PerkinElmer) the photons emitted in defined areas by the means of a grid as reference (as shown in **Fig. 1**; see **Note 9**).
5. Express luciferase activity as photon counts *per* unit of time and area ($cts/s \cdot cm^2$).

Dose-response study (see also **Note 4**):

1. Anesthetize 3 reporter mice/experimental group by gas anesthesia.
2. Injected mice i.p. with increasing concentrations (10, 25, 50 and 100 mg/kg) of D-luciferin.
3. After the time previously selected as suitable for the optimal distribution of the substrate (i.e., 15 min), take a photo of the mice and start the acquisition of the emitted photons by the means of a bioluminescence imaging system coupled with a CCD camera.
4. At the end of imaging section, perform data analysis by measuring the photons emitted in defined body areas by the means of a grid as reference (as shown in **Fig. 1**).
5. For any specific body areas, express luciferase activity as photon counts *per* unit of time and area (cts/s·cm2). Plot BLI data to establish the concentration of luciferin sufficient to carry out future studies.

3.2 *In vivo* imaging set-up: dose response analysis.

Before starting the long-term study with the different types of HRT currently in use, the study should be first done in a small number of animals to evaluate the specificity of action of the given compound in each tissue and its ability to regulate the luciferase reporter when administered orally at a dosage previously found to mimic HT in humans [34–36]. The selection of the dosage to be administered with regard to CE, BZA, and RAL is based on previous reports [35], while for the TSEC treatment a dose-response analysis with two different concentrations of BZA is performed to identify the concentration necessary and sufficient to block CE effects when used in the combined therapy. In addition, the dose-response analysis is useful to find the concentration necessary to provide the best signal-to-noise ratio in the desired target tissue (see also **Note 10**).

1. Dissolve all the compounds in DMSO and dilute them with vehicle (2% Tween 80 and 0.5% carboxymethylcellulose water solution) to final concentration (see also **Note 11**).
2. At 0900 h, treat 4-6 ERE-Luc females/experimental group *per os* (gavage) with:
    - vehicle

- 3 mg/kg CE
- 2 mg/kg BZA
- 10 mg/kg BZA
- 3 mg/kg CE + 2 mg/kg BZA
- 3 mg/kg CE + 10 mg/kg BZA
- 2 mg/kg RAL
- 10 mg/kg RAL

3. After 6 hours (see also **Note 2**), anesthetize mice by gas anesthesia.
4. Inject mice intraperitoneally (i.p.) with 80 mg/kg D-luciferin.
5. After 15 min, take a photo of the mice and start the acquisition of photon emitted by the means of a bioluminescence imaging system coupled with a CCD camera.
6. At the end of imaging section, perform data analysis by measuring the photons emitted in the areas defined in the grid shown in **Fig. 1**.
7. Express luciferase activity as photon counts *per* unit of time and area (cts/s·cm^2).
8. Plot the photon emission measured daily in the several areas as a BLI profile to assess the relative effect of the treatments in the different body areas over time (**Fig. 1**).

3.3 *In vivo* imaging set-up: identification of the sample size by power analysis.

To identify the correct sample size of the study, an initial investigation on fertile (Cyc) and ovariectomized (OVX) female ERE-Luc mice can be carried out to evaluate to which extent the lack of estrogens can affect the ER activity in a given tissue (see also **Note 12**).

1. Anesthetize 4-6 reporter mice by gas anesthesia prior to inject them intraperitoneally (i.p.) with 80 mg/kg D-luciferin.

2. 15 min after the i.p. injection, take a photo of the mice with a in dimmed light and measure photon emission. At the end of imaging section, perform data analysis by measuring the photons emitted in the areas defined in the grid shown in **Fig. 1**.
3. Express luciferase activity as photon counts *per* unit of time and area (cts/s·cm^2).
4. Plot the BLI data from specific body areas as means ± SEM and as plotted lines.

3.4 *In vivo* imaging: *spatio*-temporal analysis of long-term exposure to SERMs.

The peculiarity of reporter mice allows to monitor the activity of the reporter protein in a longitudinal day-by-day study and, therefore, to unravel the dynamics of the response to a specific compound in a tissue of interest with time. Reporter animals represent unique tools for the study of the effects of novel pharmacological treatments and for the identification of undesired effects that could be additive and dynamic, meaning that they might change with time. In virtue of their chemical structures, some substances could, indeed, accumulate in fat tissue and, once mobilized, could exert their action on whole organism by interfering with the physiological signaling of interest. Mice were housed in groups of 4 animals per cage for the duration of the study and treated daily by the selected route of administration (i.e. gavage), after having set up all the experimental conditions, including the sample size number (see also Note 1) and the dose of each treatment used (see also Note 2). In the case of the study of ER activity, it is advisable to measure bioluminescence (BLI) in the early afternoon to avoid confounding effects due to food consumption that occurs mostly during the night and is known to induce ER activity, particularly in liver [28] (see also Note 4.2).

1. After 3 weeks of ovariectomy, assign ovariectomized ERE-Luc females to a specific experimental group (8 *per* experimental groups).
2. Dissolve all the compounds in DMSO and dilute freshly with vehicle (2% Tween 80 and 0.5% carboxymethylcellulose water solution) to final concentration.
3. At 0900 h, treat ovariectomized ERE-Luc females *per os* (gavage) with:

- vehicle
- 3 mg/kg CE
- 2 or 10 mg/kg BZA
- 3 mg/kg CE + 2 or 10 mg/kg BZA (TSEC)
- 2 or 10 mg/kg RAL

4. As control, treat fertile females *per os* (gavage) with vehicle.
5. After 6 hours (at 1500 h), anesthetize mice by gas anesthesia.
6. Inject mice intraperitoneally (i.p.) with 80 mg/kg D-luciferin.
7. After 15 min, take a photo of the mice and start the acquisition of photon emitted by the means of a bioluminescence imaging system coupled with a CCD camera.
8. At the end of imaging section, perform data analysis by measuring the photons emitted in the areas defined in the grid shown in **Fig. 1**.
9. Express luciferase activity as photon counts *per* unit of time and area (cts/s·cm^2).
10. Repeat steps 2-9 daily for 21 days.
11. Plot the photon emission measured daily in the several areas as a BLI profile to assess the relative effect of the treatments in the different body areas over time (**Fig. 1**).

[Figure 1 near here]

3.5 *Ex vivo* assessment of luciferase enzymatic activity in brain areas.

During perinatal development, estrogens induce the sexual differentiation of the central nervous system (CNS) [37]. In the adult brain, estrogens, acting through their cognate receptors, that are widely expressed in the central nervous systems of both mammalian sexes [38–40], regulate several reproductive and non-reproductive functions [41–48]. With menopause, the lack of estrogens makes women more susceptible of developing neuro-inflammatory and neuro-degenerative diseases [14,15].

With the aim to evaluate the efficacy of potential HRT at the CNS level, we developed a functional method to precisely localize and quantify ER transcriptional activity in selected brain areas [49].

Analyze luciferase enzymatic activity in brain areas as following:

1. After anesthesia, perform intra cerebral ventricular (ICV) injections of 3 µl of the luciferin aqueous solution (25 mg/ml) according to specific stereotaxic coordinates (Bregma, -0.25 mm, lateral, 1 mm; depth 2.25 mm) by means of a Hamilton syringe rotated on the coronal plate of about 3° from the orthogonal position (see also **Note 13** and [50]).
2. After 20 minutes, euthanize mice and rapidly dissect brains.
3. Perform brain slices by means of a brain matrix for adult mice (coronal and sagittal, 1 mm spacing; see also **Note 3**).
4. Subject brain slices to *ex vivo* imaging session of 15 min (see also **Note 14**).
5. Quantify photon emission in selected brain areas with the dedicated software (e.g., Living Image Software for IVIS series from PerkinElmer) by superimposing over the brain areas a standardized electronic grid (as shown in shown in **Fig. 2**; the grid has been generated with the aid of a brain atlas [51]).
6. Express photon emission data as photon counts *per* unit of time and area (cts/s·mm^2).

[Figure 2 near here]

3.6 Ex vivo quantitative assessment of luciferase enzymatic activity in tissue extracts.

1. At the end of the *in vivo* imaging experiment, euthanize mice. Dissect the tissues of interest. Froze immediately the tissues on dry ice and store them at -80°C.
2. Prepare of 0.2M K-Phosphate buffer. For 100 mL, mix 90.8 mL of 1M K_2HPO_4 with 9.2 mL 1M KH_2PO_4. Keep at 4°C.

3. Prepare phosphate lysis buffer: to 25 ml of 0.2M K-Phosphate buffer, add 50 µL of 1M DTT, 1 mL of 0.2M EGTA, 0.4 mL of 0.5M EDTA. Bring volume to 50 mL with bi-distilled water. Keep at 4°C.
4. Add 300 µL of the phosphate lysis buffer to each 2 mL polyethylene microtube containing frozen tissues. Put a stainless-steel bead in each 2 mL microtube and homogenize frozen tissues (see also **Note 15**).
5. After two freezing-thawing cycles, centrifuge homogenates at 15000 rcf for 20 min 4°C.
1. Prepare LUC assay solution. For 200 mL: dissolve 104 mg of $(MgCO_3)_4Mg(OH)_2*5H_2O$ in 150 mL of bidistilled H_2O, using a magnetic stirrer (see also **Note 16**). Add 4 mL of 1M Tricin, 40 µL of 0.5M EDTA and 534 µL of 1M $MgSO_4*7H_2O$. Adjust the pH to 7.8 using HCl 1 M. Bring to 200 mL with bidistilled H_2O. Sterilize the solution by using a 0.22 µm filter. Stock the solution at 4°C.
2. Prepare LUC assay reagent. For 10 mL (enough for 100 samples): to 9.5 mL of LUC assay solution add 500 µL of 10 mM Luciferin solution (**Note 17**), 333 µL of 1M DTT (**Note 18**), 26.6 µL of 200mM ATP (**Note 19**). Mix all the components in a tube and keep the solution out of light. Store at 4°C. Before use, warm the solution to room temperature.
3. After centrifugation, transfer 20 µL of the supernatants to a white opaque 96-well plate.
4. Acquire photon emission by luminometer, with an integration time of 10 seconds, after machine-driven injecting 100 µL of LUC assay reagent.
5. Determine protein concentrations in the supernatants by performing a Bradford Protein Assay.
6. Normalize the luminescence data over protein content of each sample and express the data as relative light units (RLU) *per* µg of protein (**Fig. 3**).

[Figure 3 near here]

3.7 How to analyze the potency of a given SERM by clustering analysis.

A proper and safe HRT should be able to reinstate, in a particular tissue, the ER activity typical of the physiological condition, by avoiding the undesirable activation of ER in other tissues (such as the reproductive tissues). Previous studies performed with ERE-Luc mice demonstrated that, during the progression of the estrous cycle, the activity of ER oscillates along with time according to endogenous estrogen levels, with a photon emission profile that is specific for each tissue [6,29]. In this view, the assessment of a potency of a given compound and, potentially, of the related side-effects cannot be restrained to the mere analysis of bioluminescence raw data but should be improved through the integrative analysis of all the factors that define the pattern of ER activity under physiological conditions.

1. Upload BLI raw data obtained from an *in vivo* longitudinal study (e.g., 21 days) in a software for data analysis (e.g., GraphPad Prism). Do that for any specific body area of interest.
2. Plot BLI raw data as profiles.
3. For any body area of interest, calculate the area under the curve (AUC) and the coefficient of variation (CV%) (see also **Note 20**).
4. After doing the Fourier transform (FT) analysis (see also **Note 20**) of the profile of ER activity in time, calculate the average amplitude of cycles, estimated by measuring the degree of displacement from the resting state (calculated as the square root of the 95th percentile of the power spectra). Calculate the period of oscillation, estimated by the inverse of the frequencies under the amplitude previously calculated.
5. Perform a clustering analysis of all these values that are associated with the changes in ER activity over time by using a dedicated software (e.g., the free software available at the web page http://www.wessa.net/rwasp_hierarchicalclustering.wasp).
6. By the means of a dedicated software build a dendrogram (see also **Note 21**) showing the efficacy of selected HRTs (**Fig. 4**).

[Figure 4 near here]

4. Notes

1. Mice. Heterozygous C57BL/6 ERE-Luc [32] females 3 months of age were housed individually in ventilated plastic cages with hardwood chip bedding and animal house, fed *ad libitum* with a standard diet (4RF21 standard diet; Mucedola) and provided with filtered water. The animal room was maintained within a temperature range of 22–25C, relative humidity of 50±10%, and under an automatic cycle of 12-h light, 12-h dark (lights on at 0700 h). Mice were ovariectomized 3 weeks before the beginning of the study.

2. Influence of the diet. Animal physiology may influence *in vivo* imaging, increasing variability. For example, the fasting/feeding status has been show to strongly influence ER activation at the hepatic level [28]. The specific formula of the diet may impact on ER activation due to the variable content of phytoestrogens present in soy based diets [52]. Thus, mice must be kept under standard nutritional condition with phytoestrogen-free diets and care must be taken to avoid differential metabolic states among the experimental groups.

3. Brain slice matrices. The brain slice matrices are high-grade stainless-steel matrix useful for precise and reproducible blocking of the brain prior to sectioning. The brain slice matrices are available in two orientations: coronal (slice channels cut perpendicular to the long axis of the brain) and sagittal (slice channels cut parallel to the long axis of the brain). For this study a brain slice matrix for adult mouse (coronal and sagittal, 1 mm spacing; e.g., from Ted Pella) has been used.

4. Luciferase substrate distribution. To ensure reproducible results in the semi-quantitative *in vivo* bioluminescence imaging analysis, it is important to ensure that - in the experimental conditions adopted - the enzyme substrate (D-luciferin) reaches all organs at a concentration sufficient to saturate the enzymatic activity of the reporter [53]. Indeed, the diffusion of the substrate may change in

different mice strains and in relation of the specific formulation and route of administration used. Thus, a time-course and a dose-response study of the ability of the substrate to diffuse should be carried out. The photon emission measurement in the different body areas will enable to experimentally establish the window of time necessary to guarantee the optimal distribution of the substrate (typically 20-25 min) is selected for the dose-response study (see below).

5. Animal's fur influence. The animal's fur can influence the sensitivity of the bioluminescent signals. Mice with dark fur make detection of the photons difficult as the dark hair absorbs the luminescent signal more so than the white hair. In order to maximize luciferase detection, mice with a black fur can be eventually shaved prior to imaging.

6. Influence of anesthetic on Luciferase reaction. Given that several anesthetics can influence luciferase activity by competing for the ATP binding pocket of the enzyme, preliminary experiments should be carried out to assess whether the effects of the chosen anesthesia on photon emission are indeed negligible.

7. Luciferin IP injection. Use a 0.3 mL syringe with 30G needle to inject (IP) adult mice with D-luciferin. Make sure that the bladder or other internal organs are not penetrated by the needle.

8. At the end of each imaging session, return mice to cage and wait until they have gained consciousness and are clearly mobile before leaving unattended.

9. Quantify the BLI signal using the processing software of your BLI camera. The image software allows to quantify the signals from individual body areas by manually drawing the region of interest (ROI) over the body area of interest. Alternatively, an automatic analysis can be performed. The

values obtained can be exported directly to Microsoft Excel or other database software for data analysis and statistical data analysis.

10. Dose response analysis. Before starting the long-term study with the different types of HRT currently in use, the study should be first done in a small number of animals to evaluate the specificity of action of the given compound in each tissue and its ability to regulate the luciferase reporter when administered orally at a dosage previously found to mimic HT in humans [34–36]. The selection of the dosage to be administered with regard to CE, BZA, and RAL is based on previous reports [35], while for the TSEC treatment a dose-response analysis with two different concentrations of BZA is performed to identify the concentration necessary and sufficient to block CE effects when used in the combined therapy. In addition, the dose-response analysis is useful to find the concentration necessary to provide the best signal-to-noise ratio in the desired target tissue. This study shows the extent to which a given chemical entity is active in each target tissue and, on the other side, may provide unexpected results, by showing that a compound:

- may act in tissues where it was not supposed to exert any effect;
- may exert in some tissue an agonist and in others an antagonist activity. In order to finally elucidate its antagonist effect a given compound should be administered together with a known agonist.

This experiment allows to define the relative potency for each compound on the target in different organs and to define their action after a single administration.

11. Make a proper concentration to treat a 25g mouse with a 100 µL of compound solution.

12. Sample size by power analysis. The use of too many animals in a study is unethical and wastes animals, money, time and effort; conversely, if too few animals are used the study may lack power and miss statistical and scientific relevance. This also wastes resources and could have serious

consequences, particularly in safety assessment (for further specifications see also the web page http://www.3rs-reduction.co.uk). To identify the correct sample size of the study, an initial investigation on fertile (Cyc) and ovariectomized (OVX) female ERE-Luc mice can be carried out to evaluate to which extent the lack of estrogens can affect the ER activity in a given tissue.

Plotting the photon emission from the specific body areas as plotted lines will allow to identify the signal, the noise and the signal/noise *ratio* necessary to establish the power analysis and then the number of mice per experimental groups required to achieve the parameters described in the tab present at the web page http://www.3rs-reduction.co.uk/html/6__power_and_sample_size.html.

The profile of photon emission of Cyc ERE-Luc females changes during time in the various body areas and is ascribable to the *summa* of ligand and unliganded factors that can modulate ER activity and its downstream signaling. The physiological oscillation of ER activity in a tissue is associated with the modulation of specific target genes and pathways; the lack of estrogen signaling impairs ER activity, leading to an increased risk of developing pathologies (e.g. osteoporosis, atherosclerosis, metabolic syndrome). The search for an ideal HRT should take in consideration as a reference the oscillating ER activity showed by Cyc ERE-Luc females in some tissues (such as bone and hepatic area) and avoid to produce an increased or altered ER activation in others tissues (such as breast or uterus).

13. The injection of luciferin in the third cerebral ventricle (ICV) of anesthetized animals is done according to specific stereotaxic coordinates (bregma,−0.25 mm; lateral, 1 mm; depth, 2.25 mm) by the use of a Hamilton syringe rotated on the coronal plate about 3° from the orthogonal position.

14. *Ex vivo* imaging. Bioluminescent signal is dependent on ATP availability, which only exists in living cells. Therefore, dissected organs must be imaged immediately when removed to minimize signal loss.

15. Tissue homogenization and lysis. Add a proper volume of lysis buffer depending on the amount of tissue to be homogenized (300 of lysis buffer can be useful to process ~100-150 mg of tissue); for limited amount of tissue do not add less than 200 of lysis buffer, to avoid inefficient homogenization. Arrange the amount of lysis buffer also taking into consideration the expected signal from a specific tissue, to avoid excessive dilution that can return very low values, thus affecting the sensitivity of the analysis.

If using TissueLyzer, disruption can be generally carried out in 2 x 2 minutes shaking steps at high-speed (25–28 Hz). The homogenization can change depending on the nature of the tissue to be processed: while some tissues can be easily homogenized (soft tissues, i.e. brain), other tissues required additional steps of homogenization (hard or fibrous tissues, i.e. bone, skeletal muscle, uterus).

16. To help the dissolution of powder, it is possible to warm the solution.

17. 10 mM luciferin. Dissolve 50 mg of Firefly K salt Luciferin (MW 318.4, from Promega) in 15,7 mL of LUC Assay Solution; aliquot in tubes (1 mL), kept out of light and stock at -20° C.

18. 1M DTT. Dissolve DTT powder in bidistilled H_2O; aliquot in tubes (1 mL) and stock at -20° C.

19. 200 mM ATP. Dissolve ATP powder in 10 mL of bidistilled H_2O; aliquot in tubes (200 µl) and stock at -20° C.

20. Data analysis. The plotting and the analysis of the data can be performed by using several software programs, according to the respective user guide. In this study, GraphPad Prism Software has been used to calculate the area under the curve (AUC), the coefficient of variation (CV%), to perform the Fourier transform (FT) analysis, and to calculate the average amplitude of cycles and the

period of oscillation. FT is a mathematical transform that decomposes functions depending on time into functions depending on temporal frequency.

21. Cluster analysis The combinatorial analysis of all these measurements will return a better evaluation of the overall effects exerted by a given SERM on ER activity and may provide independent support (or contradiction) for various hypotheses about similarity and difference. The potency of a given compound should, therefore, be evaluated by performing a cluster analysis by integrating several values associated with changes in ER activity over time. In the dendrogram obtained from cluster analysis, the distances between branch lengths represent the distances between the physiology model (Cyc) and the surgical menopause model (OVX). The efficacy of each HRT is measured by its ability of a given compound to reproduce in OVX females the ER activity typical of the cycling mice: in particular, in this analysis TSEC results to reproduce an ER activation pattern more similar to Cyc than CE or other SERMs.

Funding. This work was supported by Pfizer IIRWS897258 and the ERC-Advanced Grant Ways N°322977.

Acknowledgments. We thank Clara Meda and Roberta Fontana for excellent technical support.

Figure 1

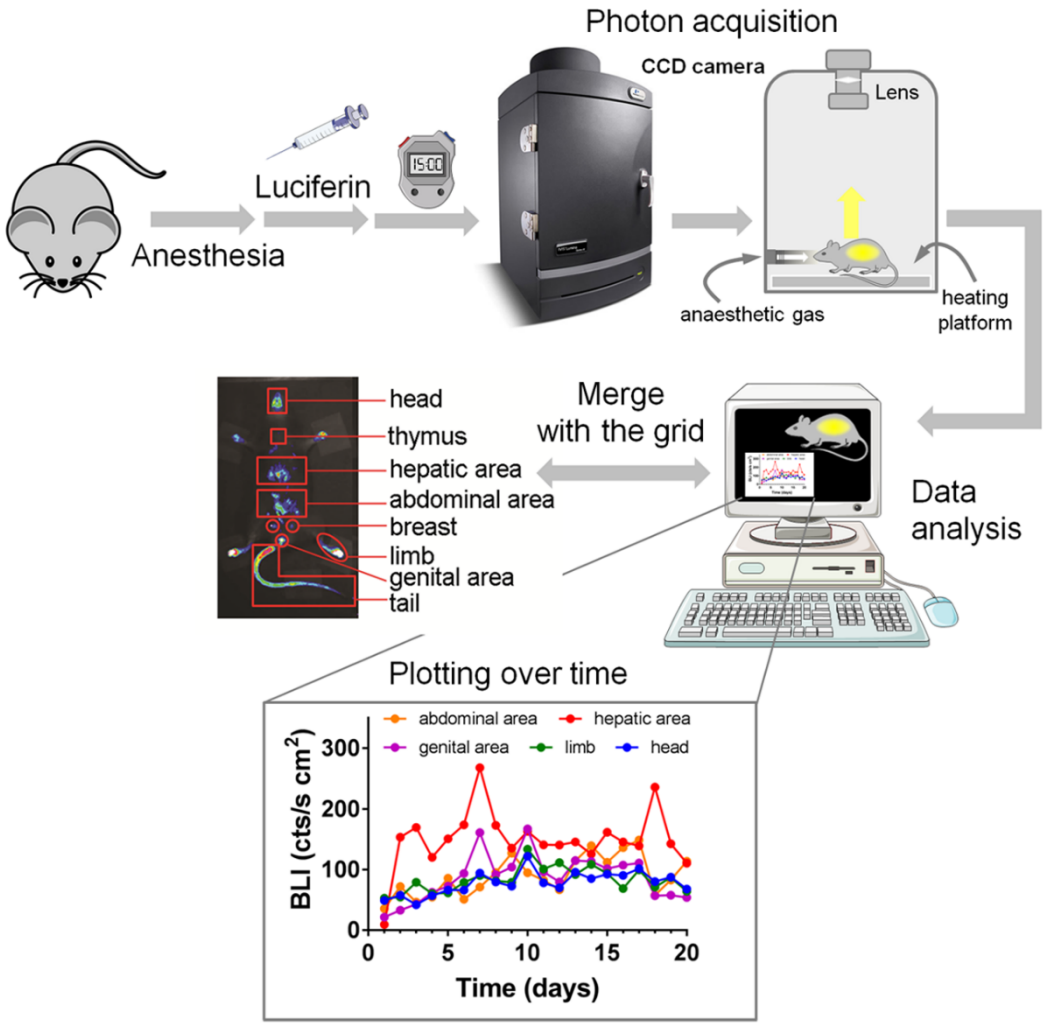

FIG. 1. *In vivo* measurement of ER activity in the ERE-Luc mouse. Intra-peritoneal injections of luciferin were performed on anesthetized mice 6 h after the treatment. After 15 min of luciferase distribution, photon emission is measured by means of a CCD camera. Semi-quantitative analysis of photon emission in selected areas was performed by merging the pseudocolor image obtained with the grid. The graph represents the profile of photon emission measured in the abdominal, hepatic, genital, limb and head areas of a single mouse during a 24 h lag-time. The emission profile represents the average pattern of ER activity in CE-treated OVX female.

Figure 2

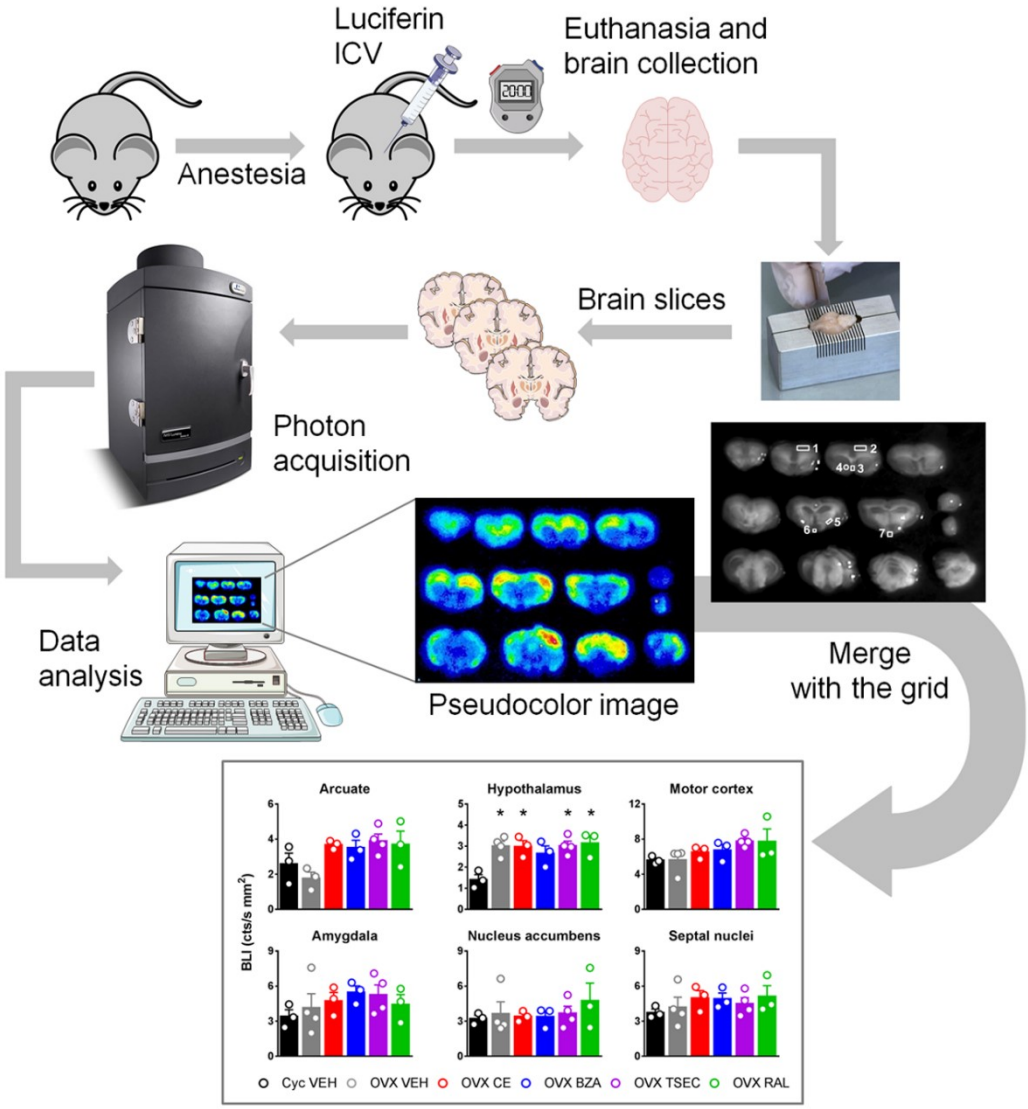

FIG. 2. Workflow of *ex vivo* imaging analysis of selected brain areas from HRT-treated ERE-Luc mice. ICV injections of luciferin were performed on anesthetized mice according to specific stereotaxic coordinates. After 20 min, mice were euthanized, and brains were sliced for bioluminescence analysis. Semi-quantitative analysis of photon emission in specific brain areas was performed by merging the pseudocolor image obtained with a grid: motor cortex (1, 2), septal nuclei (3), nucleus accumbens (4), amygdala (5), arcuate (6) and hypothalamus (7). Photon emission is expressed as counts/second/mm^2 (cts/s·mm^2). Columns represent mean ± SEM of 3-4 animals/group. *p<0.05 *vs* Cyc VEH by one-way ANOVA followed by Bonferroni *post hoc* test.

Figure 3

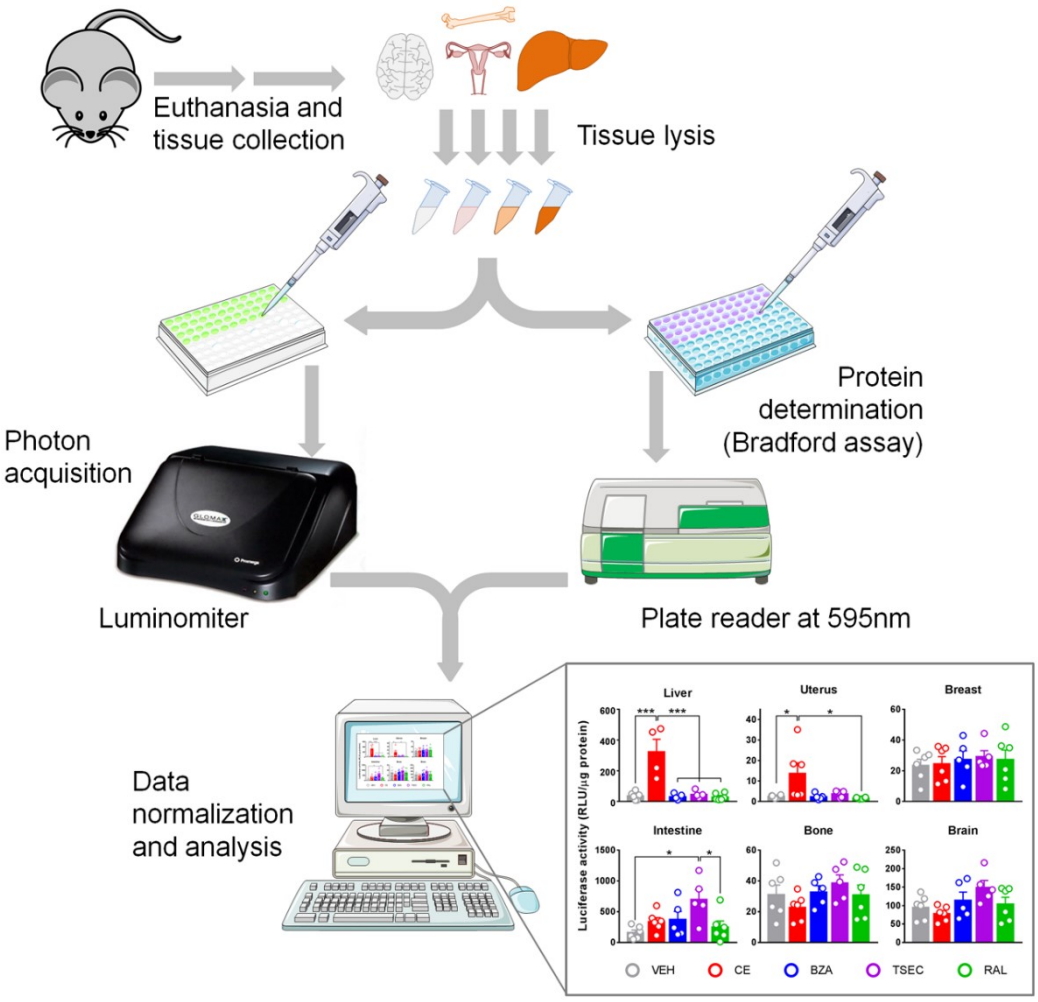

FIG. 3. Luciferase activity of ERE-Luc mice after long-term HRT. After the imaging session at day 21 of treatment, mice were euthanized and tissues rapidly dissected. Luciferase enzymatic activity was measured in tissue lysates and normalized on total protein content (RLU/µg Proteins; RLU = Relative Light Units). Columns represent mean ± SEM (n = 4-6). *p<0.05, **p<0.01 and ***p<0.001 by one-way ANOVA followed by Bonferroni *post hoc* test.

Figure 4

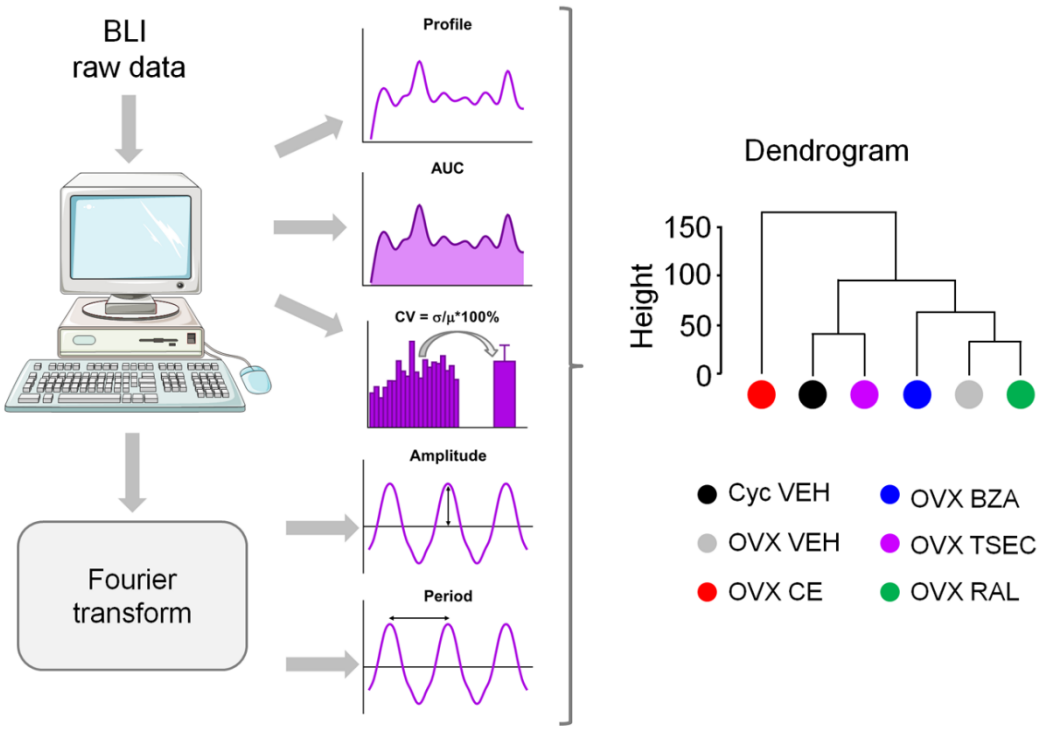

FIG. 4. Clustering analysis of photon emission of ERE-Luc mice undergoing HRT. The bioluminescence (BLI) raw data obtained in the 21 day-long study were analyzed to calculate the area under the curve (AUC), the coefficient of variation (CV%), the average amplitude of cycles and the period of oscillation. After Fourier transform (FT), the average amplitude of cycles in each group of mice is estimated by measuring the degree of displacement from the resting state (calculated as the square root of the 95th percentile of the power spectra), while the period of oscillation is estimated by the inverse of the frequencies under the amplitude previously calculated. The clustering analysis was performed with free software such as that available at the web page http://www.wessa.net/rwasp_hierarchicalclustering.wasp, which returns a dendrogram showing the efficacy of selected estrogenic compound. The distances between branches represent the distances between the physiological model (intact cycling female mice, Cyc) and the menopause model (obtained by the surgical removal of the ovaries, OVX) following treatment with conjugated

estrogens (CE), bazedoxifene (BZA), tissues selective estrogen complex (TSEC) and raloxifene (RAL). The efficacy of a given HRT is measured by its ability to mimic ER activity in Cyc mice.

References

[1] Davis, S.R., Lambrinoudaki, I., Lumsden, M., Mishra, G.D., Pal, L., Rees, M., et al., 2015. Menopause. Nature Reviews Disease Primers 1(1): 15004, Doi: 10.1038/nrdp.2015.4.

[2] Della Torre, S., 2020. Non-alcoholic Fatty Liver Disease as a Canonical Example of Metabolic Inflammatory-Based Liver Disease Showing a Sex-Specific Prevalence: Relevance of Estrogen Signaling. Frontiers in Endocrinology 11: 572490, Doi: 10.3389/fendo.2020.572490.

[3] Della Torre, S., Benedusi, V., Fontana, R., Maggi, A., 2014. Energy metabolism and fertility—a balance preserved for female health. Nature Reviews Endocrinology 10(1): 13–23, Doi: 10.1038/nrendo.2013.203.

[4] Mauvais-Jarvis, F., Manson, J.E., Stevenson, J.C., Fonseca, V.A., 2017. Menopausal Hormone Therapy and Type 2 Diabetes Prevention: Evidence, Mechanisms, and Clinical Implications. Endocrine Reviews 38(3): 173–88, Doi: 10.1210/er.2016-1146.

[5] Pinkerton, J.V., 2020. Hormone Therapy for Postmenopausal Women. New England Journal of Medicine 382(5): 446–55, Doi: 10.1056/NEJMcp1714787.

[6] Ciana, P., Raviscioni, M., Mussi, P., Vegeto, E., Que, I., Parker, M.G., et al., 2003. In vivo imaging of transcriptionally active estrogen receptors. Nature Medicine 9(1): 82–6, Doi: 10.1038/nm809.

[7] Villa, A., Della Torre, S., Stell, A., Cook, J., Brown, M., Maggi, A., 2012. Tetradian oscillation of estrogen receptor is necessary to prevent liver lipid deposition. Proceedings of the National Academy of Sciences 109(29): 11806–11, Doi: 10.1073/pnas.1205797109.

[8] Maggi, A., Della Torre, S., 2018. Sex, metabolism and health. Molecular Metabolism 15: 3–7, Doi: 10.1016/j.molmet.2018.02.012.

[9] Au, A., Feher, A., McPhee, L., Jessa, A., Oh, S., Einstein, G., 2016. Estrogens, inflammation and cognition. Frontiers in Neuroendocrinology 40: 87–100, Doi: 10.1016/j.yfrne.2016.01.002.

[10] Henderson, V.W., 2010. Action of estrogens in the aging brain: Dementia and cognitive aging. Biochimica et Biophysica Acta (BBA) - General Subjects 1800(10): 1077–83, Doi: 10.1016/j.bbagen.2009.11.005.

[11] Russell, J.K., Jones, C.K., Newhouse, P.A., 2019. The Role of Estrogen in Brain and Cognitive Aging. Neurotherapeutics 16(3): 649–65, Doi: 10.1007/s13311-019-00766-9.

[12] Benedusi, V., Meda, C., Della Torre, S., Monteleone, G., Vegeto, E., Maggi, A., 2012. A Lack of Ovarian Function Increases Neuroinflammation in Aged Mice. Endocrinology 153(6): 2777–88, Doi: 10.1210/en.2011-1925.

[13] Vegeto, E., Benedusi, V., Maggi, A., 2008. Estrogen anti-inflammatory activity in brain: A therapeutic opportunity for menopause and neurodegenerative diseases. Frontiers in Neuroendocrinology 29(4): 507–19, Doi: 10.1016/j.yfrne.2008.04.001.

[14] Vegeto, E., Villa, A., Della Torre, S., Crippa, V., Rusmini, P., Cristofani, R., et al., 2020. The Role of Sex and Sex Hormones in Neurodegenerative Diseases. Endocrine Reviews 41(2): 273–319, Doi: 10.1210/endrev/bnz005.

[15] Villa, A., Vegeto, E., Poletti, A., Maggi, A., 2016. Estrogens, Neuroinflammation, and Neurodegeneration. Endocrine Reviews 37(4): 372–402, Doi: 10.1210/er.2016-1007.

[16] Lobo, R.A., 2017. Hormone-replacement therapy: current thinking. Nature Reviews Endocrinology 13(4): 220–31, Doi: 10.1038/nrendo.2016.164.

[17] Thaung Zaw, J.J., Howe, P.R.C., Wong, R.H.X., 2018. Postmenopausal health interventions: Time to move on from the Women's Health Initiative? Ageing Research Reviews 48: 79–86, Doi: 10.1016/j.arr.2018.10.005.

[18] Cagnacci, A., Venier, M., 2019. The Controversial History of Hormone Replacement Therapy. Medicina 55(9): 602, Doi: 10.3390/medicina55090602.

[19] Rozenberg, S., Vandromme, J., Antoine, C., 2013. Postmenopausal hormone therapy: risks and benefits. Nature Reviews Endocrinology 9(4): 216–27, Doi: 10.1038/nrendo.2013.17.

[20] Genazzani, A.R., Simoncini, T., 2013. Benefits of menopausal hormone therapy—timing is key. Nature Reviews Endocrinology 9(1): 5–6, Doi: 10.1038/nrendo.2012.228.

[21] Krauss, R.M., 2002. Individualized Hormone-Replacement Therapy? New England Journal of Medicine 346(13): 1017–8, Doi: 10.1056/NEJM200203283461311.

[22] Valera, M.-C., Gourdy, P., Trémollières, F., Arnal, J.-F., 2015. From the Women's Health Initiative to the combination of estrogen and selective estrogen receptor modulators to avoid progestin addition. Maturitas 82(3): 274–7, Doi: 10.1016/j.maturitas.2015.07.012.

[23] Dahlman-Wright, K., Cavailles, V., Fuqua, S.A., Jordan, V.C., Katzenellenbogen, J.A., Korach, K.S., et al., 2006. International Union of Pharmacology. LXIV. Estrogen Receptors. Pharmacological Reviews 58(4): 773–81, Doi: 10.1124/pr.58.4.8.

[24] Krishnan, V., Heath, H., Bryant, H.U., 2000. Mechanism of action of estrogens and selective estrogen receptor modulators. Vitamins & Hormones, vol. 60. Elsevier p. 123–47.

[25] Barton, M., 2012. Position paper: The membrane estrogen receptor GPER – Clues and questions. Steroids 77(10): 935–42, Doi: 10.1016/j.steroids.2012.04.001.

[26] Prossnitz, E.R., Arterburn, J.B., 2015. International Union of Basic and Clinical Pharmacology. XCVII. G Protein–Coupled Estrogen Receptor and Its Pharmacologic Modulators. Pharmacological Reviews 67(3): 505–40, Doi: 10.1124/pr.114.009712.

[27] Pickar, J.H., Boucher, M., Morgenstern, D., 2018. Tissue selective estrogen complex (TSEC): a review. Menopause 25(9): 1033–45, Doi: 10.1097/GME.0000000000001095.

[28] Della Torre, S., Rando, G., Meda, C., Stell, A., Chambon, P., Krust, A., et al., 2011. Amino Acid-Dependent Activation of Liver Estrogen Receptor Alpha Integrates Metabolic and Reproductive Functions via IGF-1. Cell Metabolism 13(2): 205–14, Doi: 10.1016/j.cmet.2011.01.002.

[29] Della Torre, S., Biserni, A., Rando, G., Monteleone, G., Ciana, P., Komm, B., et al., 2011. The Conundrum of Estrogen Receptor Oscillatory Activity in the Search for an Appropriate Hormone Replacement Therapy. Endocrinology 152(6): 2256–65, Doi: 10.1210/en.2011-0173.

[30] Fontana, R., Della Torre, S., Meda, C., Longo, A., Eva, C., Maggi, A.C., 2014. Estrogen Replacement Therapy Regulation Of Energy Metabolism In Female Mouse Hypothalamus. Endocrinology 155(6): 2213–21, Doi: 10.1210/en.2013-1731.

[31] Rando, G., Horner, D., Biserni, A., Ramachandran, B., Caruso, D., Ciana, P., et al., 2010. An Innovative Method to Classify SERMs Based on the Dynamics of Estrogen Receptor Transcriptional Activity in Living Animals. Molecular Endocrinology 24(4): 735–44, Doi: 10.1210/me.2009-0514.

[32] Ciana, P., Di Luccio, G., Belcredito, S., Pollio, G., Vegeto, E., Tatangelo, L., et al., 2001. Engineering of a Mouse for the in Vivo Profiling of Estrogen Receptor Activity. Molecular Endocrinology 15(7): 1104–13, Doi: 10.1210/mend.15.7.0658.

[33] Aske, K.C., Waugh, C.A., 2017. Expanding the 3R principles: More rigour and transparency in research using animals. EMBO Reports 18(9): 1490–2, Doi: 10.15252/embr.201744428.

[34] Johnson, K.A., 2006. The SERM of My Dreams. The Journal of Clinical Endocrinology & Metabolism 91(10): 3754–6, Doi: 10.1210/jc.2006-1729.

[35] Peano, B.J., Crabtree, J.S., Komm, B.S., Winneker, R.C., Harris, H.A., 2009. Effects of Various Selective Estrogen Receptor Modulators with or without Conjugated Estrogens on Mouse Mammary Gland. Endocrinology 150(4): 1897–903, Doi: 10.1210/en.2008-1210.

[36] Turgeon, J.L., 2004. Hormone Therapy: Physiological Complexity Belies Therapeutic Simplicity. Science 304(5675): 1269–73, Doi: 10.1126/science.1096725.

[37] Arnold, A.P., Gorski, R.A., 1984. Gonadal Steroid Induction of Structural Sex Differences in the Central Nervous System. Annual Review of Neuroscience 7(1): 413–42, Doi: 10.1146/annurev.ne.07.030184.002213.

[38] Shughrue, P.J., Lane, M.V., Merchenthaler, I., 1997. Comparative distribution of estrogen receptor-alpha and -beta mRNA in the rat central nervous system. The Journal of Comparative Neurology 388(4): 507–25, Doi: 10.1002/(sici)1096-9861(19971201)388:4<507::aid-cne1>3.0.co;2-6.

[39] Sugiyama, N., Andersson, S., Lathe, R., Fan, X., Alonso-Magdalena, P., Schwend, T., et al., 2009. Spatiotemporal dynamics of the expression of estrogen receptors in the postnatal mouse brain. Molecular Psychiatry 14(2): 223–32, Doi: 10.1038/mp.2008.118.

[40] Weiser, M.J., Foradori, C.D., Handa, R.J., 2008. Estrogen receptor beta in the brain: From form to function. Brain Research Reviews 57(2): 309–20, Doi: 10.1016/j.brainresrev.2007.05.013.

[41] Barth, C., Villringer, A., Sacher, J., 2015. Sex hormones affect neurotransmitters and shape the adult female brain during hormonal transition periods. Frontiers in Neuroscience 9, Doi: 10.3389/fnins.2015.00037.

[42] Duarte-Guterman, P., Yagi, S., Chow, C., Galea, L.A.M., 2015. Hippocampal learning, memory, and neurogenesis: Effects of sex and estrogens across the lifespan in adults. Hormones and Behavior 74: 37–52, Doi: 10.1016/j.yhbeh.2015.05.024.

[43] Fuente-Martin, E., Garcia-Caceres, C., Morselli, E., Clegg, D.J., Chowen, J.A., Finan, B., et al., 2013. Estrogen, astrocytes and the neuroendocrine control of metabolism. Reviews in Endocrine and Metabolic Disorders 14(4): 331–8, Doi: 10.1007/s11154-013-9263-7.

[44] Galea, L.A.M., Frick, K.M., Hampson, E., Sohrabji, F., Choleris, E., 2017. Why estrogens matter for behavior and brain health. Neuroscience & Biobehavioral Reviews 76: 363–79, Doi: 10.1016/j.neubiorev.2016.03.024.

[45] Hara, Y., Waters, E.M., McEwen, B.S., Morrison, J.H., 2015. Estrogen Effects on Cognitive and Synaptic Health Over the Lifecourse. Physiological Reviews 95(3): 785–807, Doi: 10.1152/physrev.00036.2014.

[46] López, M., Tena-Sempere, M., 2015. Estrogens and the control of energy homeostasis: a brain perspective. Trends in Endocrinology & Metabolism 26(8): 411–21, Doi: 10.1016/j.tem.2015.06.003.

[47] Maggi, A., Ciana, P., Belcredito, S., Vegeto, E., 2004. Estrogens in the Nervous System: Mechanisms and Nonreproductive Functions. Annual Review of Physiology 66(1): 291–313, Doi: 10.1146/annurev.physiol.66.032802.154945.

[48] Ogawa, S., Tsukahara, S., Choleris, E., Vasudevan, N., 2020. Estrogenic regulation of social behavior and sexually dimorphic brain formation. Neuroscience & Biobehavioral Reviews 110: 46–59, Doi: 10.1016/j.neubiorev.2018.10.012.

[49] Stell, A., Belcredito, S., Ciana, P., Maggi, A., 2008. Molecular imaging provides novel insights on estrogen receptor activity in mouse brain. Molecular Imaging 7(6): 283–92.

[50] Vegeto, E., Belcredito, S., Etteri, S., Ghisletti, S., Brusadelli, A., Meda, C., et al., 2003. Estrogen receptor- mediates the brain antiinflammatory activity of estradiol. Proceedings of the National Academy of Sciences 100(16): 9614–9, Doi: 10.1073/pnas.1531957100.

[51] Paxinos, K.F.G., 2008. The Mouse Brain in Stereotaxic Coordinates, Compact 3rd Edition. Academic Press.

[52] Ciana, P., Brena, A., Sparaciari, P., Bonetti, E., Di Lorenzo, D., Maggi, A., 2005. Estrogenic Activities in Rodent Estrogen-Free Diets. Endocrinology 146(12): 5144–50, Doi: 10.1210/en.2005-0660.

[53] Biserni, A., Giannessi, F., Sciarroni, A.F., Milazzo, F.M., Maggi, A., Ciana, P., 2008. In Vivo Imaging Reveals Selective Peroxisome Proliferator Activated Receptor Modulator Activity of the Synthetic Ligand 3-(1-(4-Chlorobenzyl)-3- *t* -butylthio-5-isopropylindol-2-yl)-2,2-dimethylpropanoic acid (MK-886). Molecular Pharmacology 73(5): 1434–43, Doi: 10.1124/mol.107.042689.